IL NUOVO CIMENTO Vol. 31 C, N. 4 Luglio-Agosto 2008
DOI 10.1393/ncc/i2009-10304-1

Initial stages of oxidation at noble metal surfaces: The cases of Ag and Cu

L. Savio(*)
IMEM-CNR - Via Dodecaneso 33, 16146 Genova, Italy

(ricevuto il 13 Gennaio; approvato il 15 Gennaio 2009; pubblicato online il 2 Marzo 2009)

Summary. — The initial stages of oxide nucleation and surface oxide formation are hot topics at the moment due to the possible application of these materials in many fields of science and technology. The understanding of the parameters controlling these processes is therefore pivotal not only for the fundamental knowledge of the physical phenomenon but also for enabling the growth of better quality oxide phases, with a higher degree of order and/or a lower density of contaminants. Here I will summarize the main results obtained by a collaboration between experimental groups in Genova and Osaka and between the experimentalists in Genova and theoretical groups in Trieste and Ljubljana, on the initial oxidation of the noble metals Ag and Cu. I will show that the local morphology of surface defects and/or the dosing conditions are essential elements to determine the nature of the oxide form which starts to nucleate upon exposure to O_2. On stepped Ag we find that, under vacuum conditions, the stoichiometry of the initial oxide nuclei is tuned by the atomic geometry at the low coordination site, while on Cu(410) the oxidation efficiency comes out to be highly enhanced both by the presence of steps and by exposure to hyperthermal oxygen. The relative amount of cuprous and cupric oxide formed depends on oxidation temperature.

PACS 68.35.Ja – Surface and interface dynamics and vibrations.
PACS 68.43.Bc – *Ab initio* calculations of adsorbate structure and reactions.
PACS 79.20.Uv – Electron energy loss spectroscopy.
PACS 82.65.+r – Surface and interface chemistry; heterogeneous catalysis at surfaces.

1. – Introduction

The initial oxidation of noble and transition metal surfaces has been investigated thoroughly both theoretically [1-3] and experimentally [4,5] over the last years. Such interest is motivated by the seek of a fundamental understanding of the crossover between surface chemisorption and oxide formation and by the relevance of oxide surfaces for a wide set of

(*) E-mail: savio@fisica.unige.it

applications. Among them, I remind catalysis [6,7], the fabrication of nanoparticles with special non-linear optical properties [8] and the development of high-T_c superconductive materials [9]. Moreover, surface oxides may show catalytic and electronic properties significantly different from those of the corresponding bulk materials [10]. In spite of the many efforts, however, the phenomena governing the initial stages of oxidation are still not completely understood. Recent experimental and theoretical work [1, 11, 12] pointed out the existence of a critical coverage for the transition from chemisorbed on-surface phases to the growth of oxidic films. Carlisle *et al.* [11] proposed that the transition is determined by the steep decrease of the heat of adsorption with increasing surface coverage. Such reduction is due to the repulsive lateral interactions between adsorbates, which makes oxide formation energetically more favoured than adsorption of extra oxygen atoms at surface sites. Indeed it was demonstrated [1] that the energy gain due to oxide formation counterbalances the energetic costs of lattice deformation required for O incorporation in subsurface sites.

Ag gained relevance in this debate because the structure of the O/Ag(111) system, which was believed to consist of a surface oxide layer [13], had recently to be revised [14, 15] and assigned to a chemisorbed phase. Morever, traces of a weak surface oxide phase were observed on Ag(100) upon pre-treatment with CO [16]. On the other hand, understanding the chemistry of copper-oxygen interaction is one of the outstanding open issues of solid-state physics due to its implications in the development of high-T_c superconducting materials, whose basic units are Cu-O chains or layers [9].

Both Ag and Cu oxides exist in two stoichiometries (see fig. 1A): Me_2O (cubic) and MeO (monoclinic) (where Me stands for the general metal ion). Besides structure and stoichiometry, the two oxide phases are characterized by very different vibrational, chemical and electronic properties. Ag_2O and AgO have vibrational signatures at 525 cm^{-1} (66 meV) and 410–450 cm^{-1} (51–56 meV), respectively [17], and O atoms occupy the tetrahedral interstitials in Ag_2O and an off-centre position of the octahedral sites in AgO. Cuprous oxide (Cu_2O) is an industrially important direct-gap semiconductor with a band-gap energy of 2.17 eV [18] and it is expected to have an essentially full Cu $3d$ shell. Cupric oxide (CuO), on the other hand, has an open d shell ($3d^9$) and it is an antiferromagnetic semiconductor with an indirect gap of about 1.4 eV [19, 20]. Both Cu oxides are regarded as most promising for applications to photovoltaic cells [21-23] for which high carrier densities and low leakage currents are required to improve the performance in terms of energy conversion. Cu_2O is an efficient catalyst for the partial oxidation of propylene to acrolein [24], while CuO is used in gas sensors [25]. The synthesis of Cu_2O nanocrystals has been reported recently, further testifying the growing interest in this material [26].

Here I report on recent achievements on the initial oxidation stages of Ag and Cu under controlled, Ultra High Vacuum (UHV) conditions. Thanks to the use of stepped surfaces, *i.e.* vicinal surfaces with a high density of a well-defined undercoordinated site, I demonstrate that the geometry of the substrate and/or the dosing conditions are essential ingredients to determine the kind of oxide which initially nucleates.

2. – Experimental

All experiments were performed under controlled UHV conditions, at a base pressure better than 3×10^{-10} mbar. High Resolution Electron Energy Loss Spectroscopy (HREELS) was performed in Genova with two different experimental apparatuses. The former (I), used for most of Ag measurements, is equipped with a Quadrupole Mass Spec-

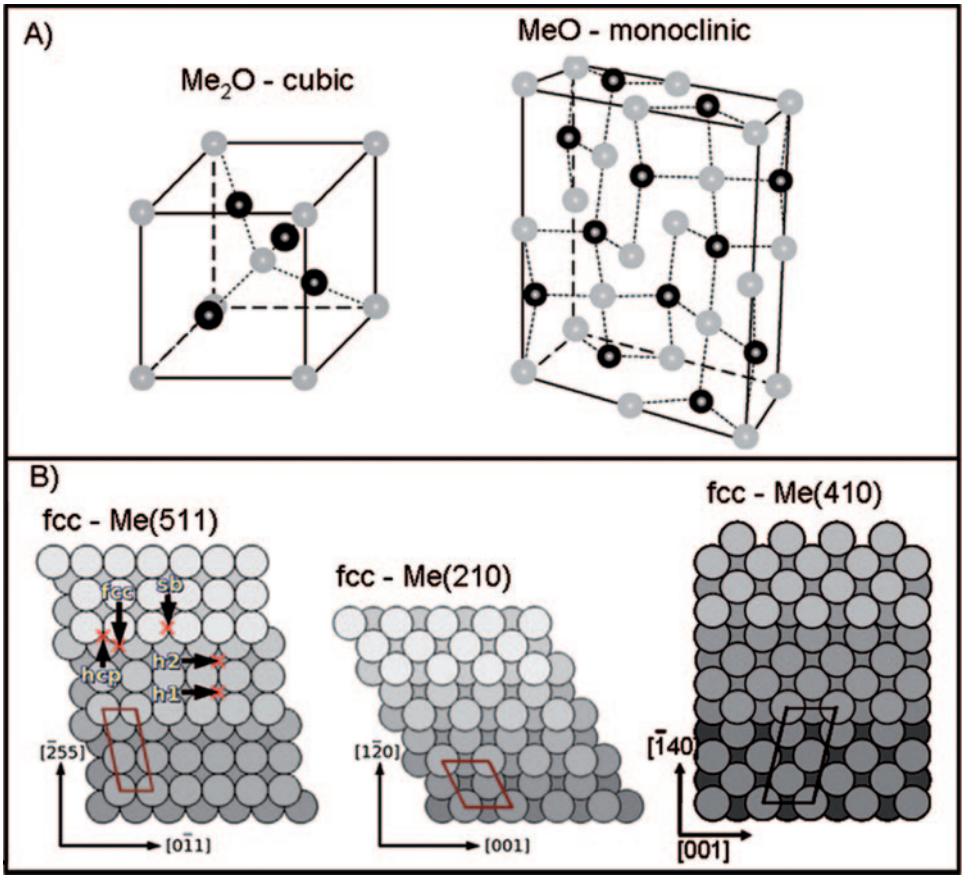

Fig. 1. – A) Structure of bulk Ag/Cu oxide in its two forms: Me2O (cubic) and MeO (monoclinic). Oxygen occupies a tetrahedral site in the former case, a distorted octahedral one in the latter. B) Schematic drawing of the stepped surfaces described in this paper. Since both bulk Ag and Cu have a fcc structure, the surface geometry is the same. The primitive unit cell and the cristallographic directions are indicated in each panel. For the (511) surface the adsorption sites investigated by theory are also marked. The lattice spacing is $a = 4.09$ Å for Ag and $a = 3.61$ Å for Cu. Me indicates the generic noble metal ion.

trometer for gas analysis, a Low Energy Electron Diffractometer (LEED), an ion gun for *in situ* cleaning of the sample, a commercial HREELS (SPECS) and a hemispherical analyser for X-ray photoemission spectroscopy (XPS - OMICRON). O_2 is dosed by backfilling the chamber. HREEL spectra are recorded in-specular, at an incidence angle $\theta_i = 62\,^\circ$ from the surface normal and with a primary electron energy $E_e = 2.0$ eV. The typical resolution is between 3.5 and 6.0 meV, depending on surface conditions. XPS spectra are acquired using a conventional $Mg_{k\alpha}$ X-ray source ($h\nu = 1253.6$ eV) and collecting the photoemitted electrons at an emission angle of $72\,^\circ$.

The second apparatus (II) was employed for measurements on Ag(210) and on Cu(410). Besides all other typical vacuum facilities, it combines a home-made HREEL spectrometer, a Cylindrical Mirror Analyzer for Auger spectroscopy and a Supersonic Molecular Beam (SMB). The typical resolution achieved in HREEL spectra is of 6–7 meV;

measurements are performed in specular, in similar conditions as for apparatus (I). O_2 is dosed either by backfilling or by SMB. In the latter case both the impact energy (E_i) and angle of incidence with respect to the surface normal (θ) are well defined.

XPS experiments on Cu(410) were performed with the surface reaction analysis apparatus (SUREAC 2000) constructed at BL23SU in SPring-8 in Japan [27]. The photon energy for recording XPS spectra was set to 1092.8 eV. In this case exposure is always performed by SMB, with O_2 seeded in helium (4% O_2). The estimated incident energy is 2.2 eV at a nozzle temperature of 1400 K. The O_2 flux at the sample position was estimated experimentally [28] to be 1.28×10^{15} molecules$\cdot$cm$^{-2}\cdot$s^{-1}, corresponding to 0.81 ML/s. (The ML is defined with respect to the unreconstructed Cu(410) substrate, $1\,\mathrm{ML} = 1.58 \times 10^{15}$ atoms/cm^2.) The surface coverage was determined from the area of the XPS spectra calibrated with respect to the $(2\sqrt{2} \times \sqrt{2})R45^\circ$ structure of Cu(100).

Ag and Cu samples are disks of 10 mm diameter, cut within 0.1° off the nominal direction, *i.e.* (210), (100) and (511) for Ag and (410) for Cu. Ag surfaces are cleaned by sputtering with 1 keV Ne ions followed by annealing to a crystal temperature $T = 740$ K, until no traces of contaminants appear in the HREEL spectra and a good surface order is detected by LEED inspection. Cu(410) is cleaned by repeated cycles of 1 keV Ar sputtering and annealing at 870 K, until no impurities were detected by SR-XPS or by Auger spectroscopy and LEED shows the sharp pattern characteristic of the pristine stepped surface. Since Ag and Cu have the same bulk fcc structure, also the geometry of the vicinal surfaces is the same. Figure 1B reports schematic drawings of the (511), (210) and (410) planes. They are all characterized by (100) nanoterraces (2, 1 and 3 atom row wide, respectively) and monatomic steps but, while in the first case the steps show a (111)-like close-packed structure, in the others they are (110)-like. On Cu(410) an STM investigation showed fuzzy steps at room temperature (RT), indicating that step roughening occurs below this T, and that the open step edges are stabilized by oxygen [29].

3. – Oxidation of stepped Ag surfaces

While the O/Ag system has been widely investigated over the past 30 years in the attempt to unravel the nature of the oxygen moiety active in the ethylene epoxidation reaction, no signatures of oxide formation were ever reported for ultra high vacuum experiments upon oxygen exposure on perfect low Miller index Ag faces [30-32] and on Ag(410) [33].

In fig. 2A I compare HREEL spectra recorded after dosing oxygen by backfilling on Ag(100) and on the vicinal surfaces Ag(511) and Ag(210). The samples were cooled down to $T = 87$ K ($T = 105$ K for Ag(210)) during the dose and then flashed to 200 K. The amount of oxygen exposed was calibrated on the basis of the adsorption probability, in order to achieve a comparable oxygen coverage on the different surfaces. For $T < 150$ K no oxygen dissociation is observed on Ag(100). On the stepped surfaces, on the contrary, dissociation is induced by steps already at low temperature [33-35]. At 200 K dissociation is complete on all surfaces. The energy loss spectrum of Ag(100) shows a single peak at 37 meV, corresponding to oxygen adatoms in the troughs of a missing row reconstructed surface [30]. Similarly, Ag(511) and Ag(210) are characterised, respectively, by a main loss at 35 meV and 39 meV. From comparison with the low Miller index surfaces and from DFT calculations, these features have been assigned, respectively, to O adatoms at the four-fold hollow sites at terraces (sites h1 and h2 in fig. 1B) on Ag(511) [35] and to oxygens decorating the steps of Ag(210) [36]. More interestingly, additional peaks at

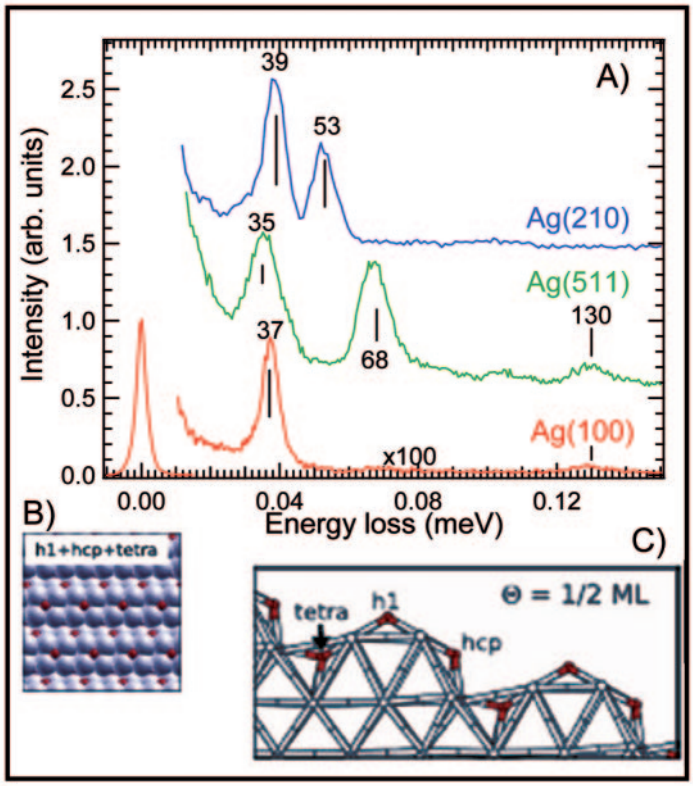

Fig. 2. – A) HREEL spectra of the Ag(100), Ag(511) and Ag(210) surfaces after exposure to O_2 at low T and annealing to 200 K. The oxide-related peaks are evident for the vicinal surfaces. Spectra were re-cooled to the 87 K (105 K) before recording the spectra. B) Top and C) side view of the first stable calculated structure with subsurface oxygen on Ag(511). The h1, hpc and distorted tetrahedral sites are occupied; the coverage is 0.5 ML.

higher frequency are present in the HREEL spectra of the stepped surfaces, at 68 meV on Ag(511) and at 53 meV on Ag(210). Such frequencies are too high for adatoms and too low for admolecules. The energy range is suitable for subsurface oxygen and the frequencies perfectly match those expected for Ag_2O and AgO, respectively [17]. Therefore the immediate information which can be gained from comparison of the behaviour of the three surfaces is that, in the presence of steps, subsurface oxygen incorporation is enabled, surface oxide nucleation is ignited in ultra high vacuum conditions and the stoichiometry of the surface oxide phase to be formed is initially tuned by the geometry of the steps: a close-packed structure favours Ag_2O while an open, (110)-like geometry allows for AgO nucleation. The oxide phase forms already at $T = 110$ K and is stable up to just below RT [34, 37]. Since the phenomenon does not occur for Ag(410), both the presence of the steps and the relaxation allowed by the very limited (100) terrace width prove to be essential. I further mention that subsurface site occupation could be monitored by high resolution XPS experiments on Ag(210), on which surface the O1*s* binding energes of super- and sub-surface species are well separated (527.9 eV *vs.* 529.6 eV [37]). This is not the case on Ag(511), which shows a main adatom peak around 530 eV [38].

For a better understanding of the oxide structure I refer to recent work by A. Kokalj, N. Bonini and co-workers, who performed *ab initio* density functional theory (DFT) calculations of the O/Ag(511) [35] and O/Ag(210) [36,39] systems. These studies confirmed that, in both cases, subsurface sites population is favoured by the strong relaxation of the surface in the presence of O adatoms at the steps; moreover, for a critical coverage $\Theta > 0.5$ ML, this phenomenon is energetically favoured with respect to the occupation of additional supersurface sites due to the strong O-O repulsion. Figures 2B and 2C show the top and side view of a stable structure at $\Theta = 0.5$ ML calculated for Ag(511). O atoms occupy the h1 and hcp on-surface sites and the distorted tetrahedral site below the first Ag layer. This structure is energetically almost degenerate (only 0.02 eV less stable) with respect to the one with adatoms only (in h1, h2 and hcp sites). For higher coverage, on the contrary, population of a distorted tetrahedral site and Ag_2O nucleation are clearly favoured. To understand the nature of the 68 meV vibration a thin $Ag_2O(311)$ oxide film commensurate with the Ag substrate was investigated theoretically, being characterized by the same kind of steps as $Ag_2O(511)$ but computationally more affordable. The theoretical results showed that the relaxed structure displays two high-energy modes at 60 and 67 meV, the latter being in good match with experimental observation. On Ag(210), on the contrary, stable subsurface occupation occurs in the octahedral interstitials and AgO nucleates. The 53 meV vibration has been nicely reproduced by theory as the in-phase displacement of O adatoms at the steps and of O atoms in the octahedral sites underneath, vibrating in a Fuchs-Kliever like motion [39].

The overall picture is therefore quite clear cut: a high density of steps favours subsurface incorporation, due to surface relaxation, and oxide nucleation. The nature of the subsurface site to be populated and the stoichiometry of the surface oxide phase to be formed are initially tuned by the geometry of the steps: a (111)-like structure favours occupation of distorted tetrahedral sites and Ag_2O nucleation, while open steps lead to incorporation into octahedral interstitials and to AgO formation.

4. – Oxidation of Cu(410)

As mentioned in the introduction section, Cu oxide, in its two forms, has important applications in high-T_c superconductivity, in the development of photovoltaic cells and as a catalyst. The growth of ordered thin oxide layers with a low degree of contamination is therefore mandatory to improve the efficiency of Cu oxide based devices.

Ordered Cu_2O and CuO films and nanostructures are usually grown by controlling O_2 pressure and substrate temperature during deposition. Figure 3 reports a HREEL spectrum recorded after exposure of Cu(410) at 500 K to 3000 L of O_2 by backfilling the chamber. Oxide formation is witnessed by the losses at 78 and 19 meV, while the 38 meV peak is associated to chemisorbed oxygen. High temperature and high doses are required; the oxidation efficiency is low, but higher than for Cu(111) and Cu(110) [40,41], while I recall that no oxidation of Cu(100) was ever observed in UHV [42]. Therefore, also in this case, the high density of low coordinated sites favors oxygen incorporation and oxide formation.

The use of hyperthermal O_2 molecular beams may improve the quality of the grown thin films, as demonstrated, *e.g.*, for organic films [43]. Moreover it allows to produce the oxide at lower crystal temperatures, avoiding contamination problems and reducing film defectivity. Collision-induced absorption (CIA) [44] and local heating of the substrate were indeed shown to be effective in inducing oxide nucleation [45], opening up new possibilities for the production of nanostructured oxides. This technique has been successfully applied for oxidation of low Miller index Cu surfaces [27, 46, 47].

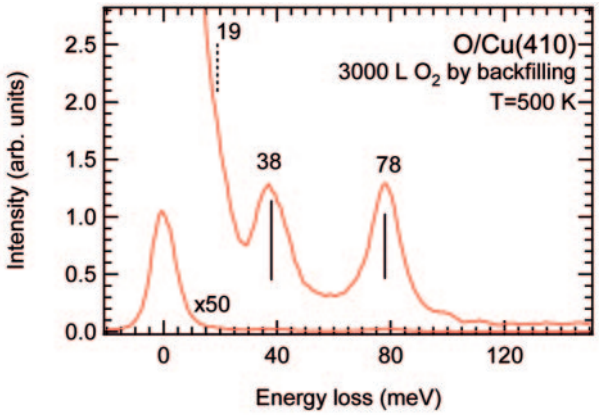

Fig. 3. – HREEL spectrum of the oxidised Cu(410) surface. Oxide-related vibrations are at 78 meV and 19 meV (almost embedded in the elastic tail).

Here I report on results for Cu(410). Cu(410) is the stable faceting observed after massive oxygen exposure on Cu(100) [48]; furthermore, under-coordinated sites are expected to act as nucleation centers and open up efficient pathways for the incorporation of hyperthermal O atoms [34].

In fig. 4, I compare XPS spectra, recorded by my Japanese collaborators at Spring 8, of the Cu(410) surface exposed to a 2.2 eV O_2 beam at normal incidence: in panel A the substrate is at 300 K during the dose, in panel B it is at 100 K. The achieved oxygen coverage is similar in the two cases but, from the peak-shape analysis of the O1*s* spectra, it is evident that different oxygen species are present and that they are populated in different amounts in the two experiments. The O1*s* peaks are fitted with a Voigt function with parameters G and Lorentzian width Γ. The peak-fitting procedure was performed using Unifit2002 software [49] and subtracting the Shirley background [50].

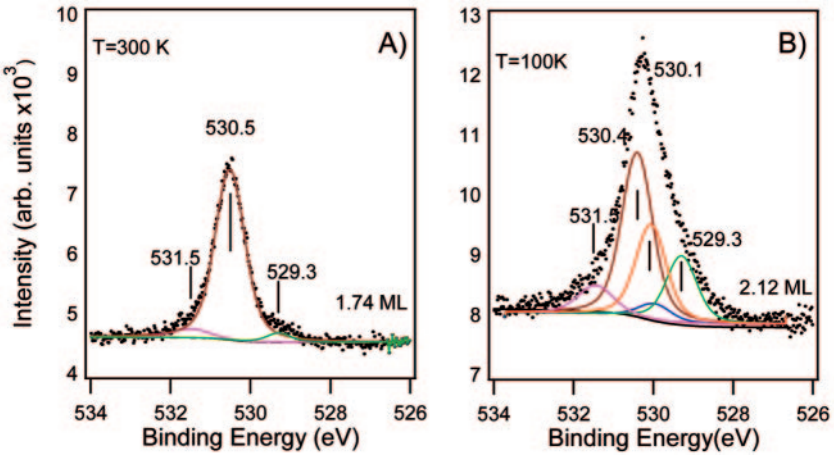

Fig. 4. – SR-XPS spectra of the Cu(410) surface previously exposed to a 2.2 eV O_2 SMB at normal incidence. Raw data (dotted curves) and deconvolved components (continuous lines) are shown. Panel A) dose performed at RT; panel B) dose performed at 100 K.

Comparing the results obtained for the two temperatures it is evident that:

a) At RT the XPS intensity is resolved into three components, corresponding to Cu_2O ($G = 0.68\,\text{eV}$, $\Gamma = 0.35\,\text{eV}$) at 530.5 eV, to a small CuO peak ($G = 0.50\,\text{eV}$, $\Gamma = 0.35\,\text{eV}$) at 529.3 eV [51] and to an additional contribution at 531.5 eV ($G = 0.87\,\text{eV}$, $\Gamma = 0.35\,\text{eV}$), probably due to O adatoms chemisorbed on Cu oxide [40]. At this, relatively high, O concentration the chemisorbed oxygen signal at 530.1 eV is no longer present, witnessing that the substrate is now fully covered by Cu_2O. A small amount of CuO was also reported for Cu_2O formation on Cu(110) [41].

b) At $T = 100\,\text{K}$ five O species are present, corresponding to Cu_2O, CuO, chemisorbed oxygen on metal ($G = 0.76\,\text{eV}$, $\Gamma = 0.36\,\text{eV}$), chemisorbed oxygen on oxide and a further, subsurface oxygen species at 530.1 eV ($G = 0.71$, $\Gamma = 0.35\,\text{eV}$).

c) The relative weight of the O1s components at 100 K and at 300 K is totally different. At room temperature the 2.2 eV SMB produces almost only Cu_2O, while at low T significant amounts of CuO and of subsurface oxygen are present. This is also confirmed by Auger experiments and by quantitative analysis of the oxygen uptakes [52]. This result suggests that the local heating produced by the hyperthermal O_2 beam is insufficient for the formation of a homogeneous Cu_2O layer. Mobility of Cu and O atoms, attained at higher T only, is thus required. Anyway, CuO nucleation at low T is surprising since this moiety is usually produced at high T and high O_2 pressure [53, 54]. It is proposed that, under the present conditions, Cu_2O may form following the route $CuO + Cu \rightarrow Cu_2O$, with the CuO phase acting as a metastable precursor. It should be noted that a similar reaction pathway, leading to Cu_2O formation, occurs when depositing Cu atoms on CuO thin films [55]. Indeed, when heating to 273 K, the O1s component at 529.3 eV disappears, indicating the metastable nature of the cupric oxide phase. This process is of general importance for the fabrication of metastable phases of interest for the synthesis of suboxides [56] and of new nanostructured materials [57].

d) At low T the introduction of a contribution at 530.1 eV, corresponding to subsurface oxygen, is necessary to fit the data. This binding energy nearly coincides with the one of chemisorbed oxygen, but the introduction of a new species is justified because: i) it corresponds to a significant reduction of the χ^2 value per degree of freedom (from 1.64 to 1.54); ii) if only chemisorbed oxygen corresponded to the 530.1 eV intensity, its weight would be close to 0.5 ML, *i.e.* close to the saturation coverage. As a consequence, only a very small fraction of the surface would be covered by the oxide, which consists then of 3-dimensional islands unphysically elongated normally to the surface.

The present data clearly show that nearly perfect Cu oxide films can be grown on Cu(410) by hyperthermal O_2 beam exposure. The efficiency of oxide formation increases strongly with O_2 translational energy, allowing to produce the oxide already at room temperature and even at $T \sim 100\,\text{K}$ for 2.2 eV O_2 beams. In the former case almost only Cu_2O is detected, while also CuO forms at $\sim 100\,\text{K}$. The relative amount of the two oxide phases is therefore tuned by dosing conditions and substrate temperature.

At this point it is worth spending a few words on the oxidation mechanism. In view of the Cu(410) stepped geometry, it could be due either to collision-induced adsorption or to the detachment of Cu atoms from the steps, which would act as additional O_2 dissociation and oxide nucleation centers, as in the case of Cu(110). In the former hypothesis

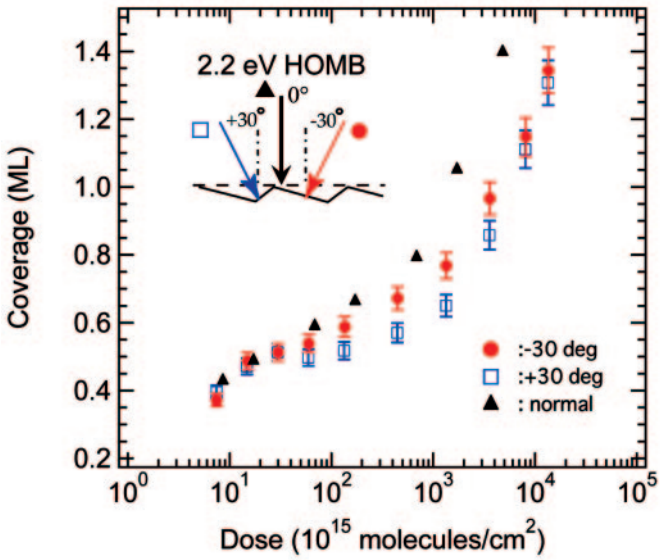

Fig. 5. – O uptake curves for 2.2 eV O_2 SMB on Cu(410) at room temperature, parametric in angle of incidence. The geometry of the surface and the angles of incidence corresponding to the three series of data are shown in the inset.

oxidation is expected to be more efficient for normal incidence of the O_2 beam on the surface, while in the latter grazing incidence on the step edges should be the privileged condition. Figure 5 reports the oxygen coverage *vs.* exposure, as estimated from XPS spectra recorded at the Spring 8 Synchrotron Radiation Source, for the hyperthermal O_2 beam impinging at different angles on the surface. As is evident, there is little difference in the oxidation efficiency for beams hitting the surface at $-30\,^\circ$ and $+30\,^\circ$, *i.e.* grazing and nearly normal to the steps. On the contrary, above the critical coverage of 0.5 ML, at which oxide starts to nucleate, the amount of oxygen detected is maximum for normal incidence. This allows to suggest that oxidation occurs via a collision-induced mechanism (CIA) [58], as is the case also for Cu(100). A semi-quantitative rate equation model has been developed to reproduce experimental data on the basis of a CIA oxidation process [58].

5. – Conclusions

In this paper I have shown how the initial oxidation stages of Ag and Cu can be tuned by surface geometry and/or exposure conditions. On Ag, the formation of AgO or Ag_2O nuclei, with O populating the octahedral interstitials or distorted tetrahedral sites, respectively, is determined by the open or closed geometry of the steps. On Cu, the presence of open steps increases the oxidation rate but, when dosing oxygen with a SMB, the relative amount of cuprous and cupric oxide to be formed strongly depends on substrate temperature.

* * *

The author thanks L. Vattuone, M. Rocca, C. Giallombardo, and A. Gerbi for collaboration in the experimental work performed in Genova, N. Bonini,

A. Dal Corso and S. de Gironcoli (SISSA, Trieste) for calculations on Ag(210), A. Kokalj (Jožef Stefan Institute, Ljubljana, Slovenia) for calculations on Ag(511) and M. Okada (PRESTO, Japan Science and Technology Agency) and K. Moritani (Synchrotron Radiation Research Center, Japan Atomic Energy Agency) for experimental work on Cu(410).

REFERENCES

[1] Todorova M., Li W. X., Ganduglia-Pirovano M. V., Stampfl C., Reuter K. and Scheffler M., *Phys. Rev. Lett.*, **89** (2002) 96103.
[2] Li W. X., Stampfl C. and Scheffler M., *Phys. Rev. B*, **67** (2003) 045408.
[3] Michaelides A., Bocquet M. L., Sautet P., Alavi A. and King D. A., *Chem. Phys. Lett.*, **367** (2003) 344.
[4] Schmidt M., Masson A. and Brechignac C., *Phys. Rev. Lett.*, **91** (2003) 243401.
[5] Waterhouse G. I. N., Bowmaker G. A. and Metson J. B., *Appl. Surf. Sci.*, **183** (2001) 191.
[6] Over H. *et al.*, *Science*, **287** (2000) 1474.
[7] Hendriksen B. L. M. and Frenken J. W. M., *Phys. Rev. Lett.*, **89** (2002) 046101.
[8] Chiu Y., Rambabu U., Hsu Ming-Hong, Shieh Han/Ping D., Chen Chien-Yang and Lin His Hsiang, *J. Appl. Phys.*, **94** (2003) 1996.
[9] Waldram J. R., *Superconductivity of Metals and Curprates* (IOP Publishing Ltd, London, UK) 1996.
[10] Freund H. J. *et al.*, *Rep. Prog. Phys.*, **59** (1996) 283
[11] Carlisle C. I., Fujimoto T., Sim W. S. and King D. A., *Surf. Sci.*, **470** (2000) 15.
[12] Kokalj A., Dal Corso A., de Gironcoli S. and Baroni S., *J. Phys. Chem. B*, **110** (2006) 367.
[13] Schnadt J., Michaelides A., Knudsen J., Vang R. T., Reuter K., Lægsgaard E., Scheffler M. and Besenbacher F., *Phys. Rev. Lett.*, **96** (2006) 146101.
[14] Schmid M., Reicho A., Stierle A., Costina I., Klikovits J., Kostelnik P., Dubay O., Kresse G., Gustafson J., Lundgren E., Andersen J. N., Dosch H. and Varga P., *Phys. Rev. Lett.*, **96** (2006) 146102.
[15] Li W.-X., Stampfl C. and Scheffler M., *Phys. Rev. B*, **68** (2003) 165412.
[16] Rocca M. *et al.*, *Phys. Rev. B*, **63** (2001) 081404(R).
[17] Pettinger B. *et al.*, *Angew. Chem. Int. Ed.*, **33** (1994) 85.
[18] Baumeister P. W., *Phys. Rev.*, **121** (1961) 359.
[19] Koffyberg F. P. and Benko F. A., *J. Appl. Phys.*, **53** (1982) 1173.
[20] Filippetti A. and Fiorentini V., *Phys. Rev. Lett.*, **95** (2005) 086405.
[21] Olsen L. C., Addis F. W. and Miller W., *Sol. Cells*, **7** (1982) 247.
[22] Pollack G. P. and Trivich D., *J. Appl. Phys.*, **46** (1975) 163.
[23] Ray S. C., *Sol. Energy Mater. Sol. Cells*, **68** (2001) 307.
[24] Reitz J. B. and Solomon E. I., *J. Am. Chem. Soc.*, **120** (1998) 11467.
[25] Ishihara T., Higuchi M., Takagi T., Ito M., Nishiguchi H. and Takita T., *J. Mater. Chem.*, **8** (1998) 2037.
[26] Zhou G.-W. and Yang J. C., *Surf. Sci.*, **531** (2003) 359; *Phys. Rev. Lett.*, **93** (2004) 226101; Zhou G.-W., Slaughter W. S. and Yang J. C., *Phys. Rev. Lett.*, **94** (2005) 246101.
[27] Okada M., Moritani K., Goto S., Kasai T., Yoshigoe A. and Teraoka Y., *J. Chem. Phys.*, **119** (2003) 6994.
[28] Teraoka Y. and Yoshigoe A., *Jpn. J. Appl. Phys.*, **41** (2002) 4253.
[29] Knight P. J., Driver S. M. and Woodruff D. P., *Chem. Phys. Lett.*, **259** (1996) 503.
[30] Rocca M. *et al.*, *Phys. Rev. B*, **61** (2000) 213.
[31] Vattuone L. *et al.*, *J. Chem. Phys.*, **101** (1995) 713.

[32] Loffreda D. *et al.*, *Surf. Sci.*, **530** (2003) 26. The paper reports on a complete HREELS and DFT investigation of the vibrational modes of O/Ag(100). We observed a tiny loss at 67 meV, tentatively assigned to the parallel vibration of O predicted at 59 meV. Such assignment must now be revised and the loss attributed to oxide nucleation at defects. Close-packed steps are indeed expected to be the most common defect at Ag(100).
[33] Savio L., Vattuone L. and Rocca M., *Phys. Rev. Lett.*, **87** (2001) 276101.
[34] Vattuone L., Savio L. and Rocca M., *Phys. Rev. Lett.*, **90** (2003) 228302.
[35] Savio L., Giallombardo C., Vattuone L., Kokalj A. and Rocca M., *Phys. Rev. Lett.*, **101** (2008) 266103.
[36] Kokalj A., Bonini N., Dal Corso A., de Gironcoli S. and Baroni S., *Surf. Sci.*, **566-568** (2004) 1107.
[37] Savio L. *et al.*, *J. Phys. Chem. B*, **110** (2006) 942.
[38] Savio L. *et al.*, *J. Phys.: Condens. Matter*, **20** (2008) 224006.
[39] Bonini Nicola, Dal Corso Andrea, Kokalj Anton, de Gironcoli Stefano and Baroni Stefano, *Surf. Sci.*, **587** (2005) 50.
[40] Dubois L. H., *Surf. Sci.*, **119** (1982) 399.
[41] Baddorf A. P. and Wendelken J. F., *Surf. Sci.*, **256** (1991) 264.
[42] Sexton B. A., *Surf. Sci.*, **88** (1979) 299.
[43] Casalis L., Danisman M. F., Nickel B., Bracco G., Toccoli T., Iannotta S. and Scoles G., *Phys. Rev. Lett.*, **90** (2003) 206101.
[44] Vattuone L., Gambardella P., Burghaus U., Cemic F., Valbusa U. and Rocca M., *J. Chem. Phys.*, **109** (1998) 2490.
[45] Okada M., Hashinokuchi M., Fukuoka M., Kasai T., Moritani K. and Teraoka Y., *Appl. Phys. Lett.*, **89** (2006) 201912.
[46] Moritani K. *et al.*, *J. Vac. Sci. Technol. A*, **22** (2004) 1625.
[47] Moritani K. *et al.*, *Eur. Phys. J. D*, **38** (2006) 111.
[48] Bouilliard J. C., Domange J. L. and Sotto M., *Surf. Sci.*, **8** (1967) 223.
[49] `http://www.uni-leipzig.de/~unifit/`.
[50] Shirley D. A., *Phys. Rev. B*, **5** (1972) 4709.
[51] Ghijsen J., Tjeng L. H., van Elp J., Eskes H. and Czyzyk M. T., *Phys. Rev. B*, **38** (1988) 11322.
[52] Okada M., Vattuone L., Moritani K., Savio L., Teraoka Y., Kasai T. and Rocca M., *Phys. Rev. B*, **75** (2007) 233413.
[53] Kauur M., Muthe K. P., Despande S. K., Choudhury S., Singh J. B., Verma N., Gupta S. K. and Yakhmi J. V., *J. Cryst. Growth*, **289** (2006) 670.
[54] Muthe K. P., Vyas J. C., Narang S. N., Aswal D. K., Gupta S. K., Bhattacharya D., Pinto R., Kothiyal G. P. and Sabharwal S. C., *Thin Solid Films*, **324** (1998) 37.
[55] Wu M. C. and Møller P. J., *Phys. Rev. B*, **40** (1989) 6063.
[56] Kim J. Y. *et al.*, *J. Am. Chem. Soc.*, **125** (2003) 10684.
[57] Liu B. and Zeng H. C., *J. Am. Chem. Soc.*, **126** (2004) 8124.
[58] Okada M., Vattuone L., Gerbi A., Savio L., Rocca M., Moritani K., Teraoka Y. and Kasai T., *J. Phys. Chem. C*, **111** (2007) 17340.